

Transient Networks by ABA Triblock Copolymers and Microemulsions: A Rheological Study

M. Odenwald, H.-F. Eicke,* and W. Meier

Institut für Physikalische Chemie, Departement Chemie der Universität,
CH-4056 Basel, Switzerland

Received February 2, 1995; Revised Manuscript Received April 11, 1995*

ABSTRACT: The rheological properties of microemulsion–triblock copolymer [poly(oxyethylene)-*b*-polyisoprene-*b*-poly(oxyethylene)] transient networks were studied by oscillatory shear measurements. The chemical nature of the surfactants (ionic or nonionic) seems not to affect the principal viscoelastic feature of our systems. The main differences between both systems are caused by the individual phase behavior of the underlying microemulsions: within a particular temperature region the temperature dependences of the mechanical properties are opposite for ionic and nonionic systems. Also, specific interactions between the surfactants and the hydrophilic poly(oxyethylene) blocks of the network links lead to a significant effect on the formation of network structures and on the lifetimes of network cross-links. These lifetimes are connected with characteristic relaxation times derived from the mechanical spectra. Model considerations yielded the definition of a persistence length of the triblock copolymer molecules dissolved in microemulsions.

Introduction

The fundamental characteristic of emulsions, particularly thermodynamically stable microemulsions, is to consist of domains of grossly different physical properties, i.e., water and oil. In a certain range of their phase diagrams the structure of water-in-oil microemulsions is characterized by nanometer-sized water droplets covered by a monomolecular surfactant layer in an oil continuum.¹ We report on ionic microemulsions formed by sodium bis(2-ethylhexyl)sulfosuccinate (=AOT)/water/isooctane and nonionic microemulsions formed by pentakis(ethylene glycol)–mono(tetradecyl ether) (C₁₄E₅)/water/*n*-octane. The number (*n*) and diameter (*d*) of the aqueous nanodroplets are determined by weighed-in amounts of surfactant, water, and oil. Typical values for the microemulsions are $d = 1.5 \times 10^{-8}$ m and $n = 3.9 \times 10^{16}$ cm⁻³.

Due to their compartmental structure water-in-oil microemulsions are considered to be “complex solvents” for ABA triblock copolymers containing hydrophilic poly(oxyethylene) blocks (POE) and a lipophilic polyisoprene midblock (PI). One can imagine that such polymers can form mesophases in microemulsions by incorporating their hydrophilic POE blocks into the aqueous cores of the nanodroplets and by bridging the water domains via their oil-soluble PI midblocks (see Figure 1). Above a certain polymer concentration a three-dimensional polymer–microemulsion network having the typical physical properties of transient networks is formed.^{2,3}

Apart from their transient network properties, a particularly interesting feature of our systems is that the microemulsions keep their characteristics: the phase behavior of the microemulsions is qualitatively preserved, e.g., the reversible aggregation of nanodroplets and phase transition to lyotropic liquid crystalline phases. This observation helps us to interpret the mechanical properties of the transient networks.

Moreover, material exchange between individual nanodroplets, especially the exchange of hydrophilic POE blocks as constituents of cross-links within the transient network, is essentially determined by the droplet–droplet contact time. The latter is strongly dependent

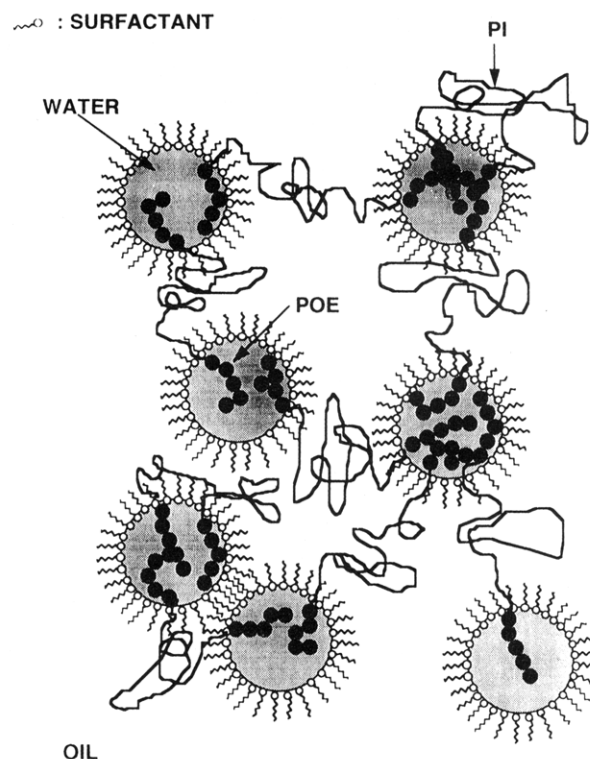


Figure 1. Triblock copolymers forming a transient network in a water-in-oil microemulsion.

on the microemulsion's composition. Consequently, the lifetimes of the cross-links are related to the phase behavior of the complex fluids.

It is anticipated that water-in-oil microemulsions interact in a characteristic manner with ABA triblock copolymers depending on the chemical nature of the surfactant, i.e., ionic or nonionic. From previous work⁴ we know that nanodroplets covered by ionic surfactants require relatively large amounts of polymers in order to form three-dimensional transient networks. Nonionic surfactant microemulsions, in contrast, show the same properties at much smaller polymer concentrations.

In this paper we report on transient networks formed by pentakis(ethylene glycol)–mono(tetradecyl ether) (C₁₄E₅)/water/*n*-octane (nonionic system, “nio”) and

* Abstract published in *Advance ACS Abstracts*, June 1, 1995.

Table 1. Molecular Weights of the POE-PI-POE Triblock Copolymers

polymer	$M_w(\text{PI})$	$M_w(\text{PEO})$	M_w/M_n
TBC6	50 000	10 000	1.015
TBC8	50 000	5 000	1.015

AOT/water/isooctane (ionic system, "io") microemulsions containing poly(oxyethylene)-*b*-polyisoprene-*b*-poly(oxyethylene) triblock copolymers. Results of rheological investigations on these systems are reported.

Experimental Section

Material. Water-in-oil microemulsions were prepared by the nonionic surfactant pentakis(ethylene glycol)-mono(tetradecyl ether) (C_{14}E_5) or by the ionic surfactant sodium bis-(2-ethylhexyl)sulfosuccinate (AOT). Both surfactants were obtained from Fluka in the highest grade available and used without further purification, likewise *n*-octane and isooctane (puriss.). Water was deionized with an Alpha-Q reagent-grade system from Millipore.

Both poly(ethylene oxide)-*b*-polyisoprene-*b*-poly(ethylene oxide) triblock copolymers TBC6 and TBC8 (see Table 1) were synthesized via anionic polymerization:

The isoprene monomer was purified by stirring with CaH_2 overnight and then distilled under N_2 and stored at -20°C prior to use. A last purification step, carried out immediately before the polymerization, used high-vacuum purification techniques with phenylmagnesium chloride as a drying agent. The purified monomer was recondensed to an ampule, which was then filled with a slight overpressure of dry N_2 . Ethylene oxide was purified by the same procedure.

The polymerization was carried out in a stirred glass reactor under purified N_2 . Tetrahydrofuran, used as a solvent for the polymerization, was purified by refluxing and distilling over sodium benzophenone adduct. The polymerization of isoprene was initiated with potassium naphthalide at -30°C . After 2 h, a sample was removed from the reactor to characterize the polyisoprene midblock. Ethylene oxide was then added, resulting in a considerable increase in the viscosity of the solution. After a half hour, the temperature was gradually increased to 60°C , and the ethylene oxide was left to polymerize overnight. The reaction was then terminated with distilled water and the polymer recovered by precipitation in hexane.

Residual naphthalene (from the initiator) and a small amount (<5%) of isoprene homopolymer were extracted from the product by soaking in hexane, followed by centrifugation of the gelatinous mass.

The polymer-containing microemulsions were prepared by mixing weighed amounts of microemulsions with varying amounts of polymers and stirring the mixtures at 35°C (io) or 20°C (nio) for several days. Mass fractions of the droplets are given by

$$c_w = \frac{m_s + m_w}{m_s + m_w + m_o} \quad (1)$$

with $m_x \approx$ mass of surfactant ($x = s$), water ($x = w$), and oil ($x = o$). The droplet size is a function of

$$r_w = m_w/m_s \quad (2)$$

The amount of polymer is given by the number ratio $R \approx$ (polymer molecules/water droplet). Polymer concentrations ranged from 1.80×10^{-3} ($R = 3$) to 0.116 g ($R = 20$) of TBC6/ cm^3 of microemulsion (io) and from 5.20×10^{-3} ($R = 1$) to $2.08 \times 10^{-2} \text{ g}$ ($R = 4$) of TBC8/ cm^3 of microemulsion (nio) (see Table 2).

Measurements. In order to evaluate the mechanical properties of microemulsion-triblock copolymer systems, rheological measurements were performed. They were carried out with a Carrired CRSH 100 controlled stress rheometer, combined with a homemade cone-cone geometry ($3.5 \times 10^{-5} \text{ m}$ gap, corrected for thermal expansion) and a thermostable

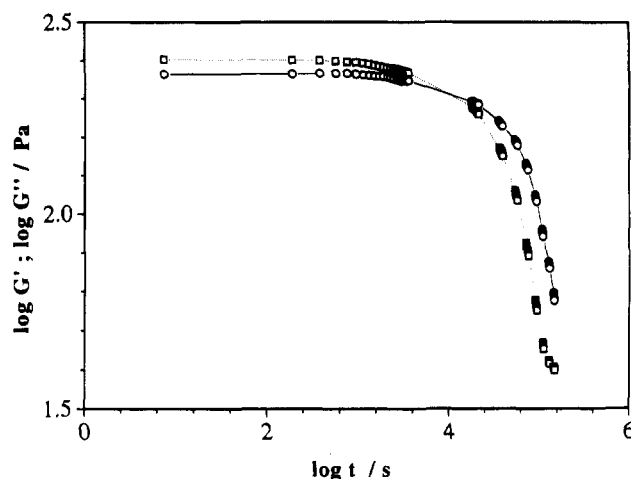


Figure 2. Time sweep ($\nu = 1 \text{ Hz}$, $T = 18^\circ\text{C}$) to illustrate limited stability of an ionic microemulsion sample (polymer concentration: $R = 12$): (—○—) G' ; (—□—) G'' .

Table 2. Composition of the Triblock Copolymer-Microemulsion Systems

sample	surfactant	polymer	R	c_w	r_w
A1	AOT	TBC6	3	0.35	2.50
A2	AOT	TBC6	4	0.35	2.50
A3	AOT	TBC6	6	0.35	2.50
A4	AOT	TBC6	8	0.35	2.50
A5	AOT	TBC6	12	0.35	2.50
A6	AOT	TBC6	20	0.35	2.50
B1	C_{14}E_5	TBC8	1	0.25	2.00
B2	C_{14}E_5	TBC8	2	0.25	2.00
B3	C_{14}E_5	TBC8	3	0.25	2.00
B4	C_{14}E_5	TBC8	4	0.25	2.00

cap ($\pm 0.05 \text{ K}$) to isolate samples from the outer atmosphere and prevent solvent evaporation (for a detailed description, see ref 4).

The storage modulus $G'(\omega)$ and loss modulus $G''(\omega)$ were measured in the frequency range $0.628 \text{ s}^{-1} \leq \omega \leq 251.3 \text{ s}^{-1}$ at various temperatures and strain amplitudes of about 3%. A relative narrow frequency range had to be chosen because of limited sample stability in the rheometer. In Figure 2 the plots of G' and G'' of an ionic sample ($R = 12$) are shown during a time sweep at $T = 18^\circ\text{C}$ and $\nu = 1 \text{ Hz}$. From this figure it can be seen clearly that the sample is stable for only about 1 h because the measuring unit could not be tightened completely in spite of all precautions taken.

Using the isotherms, master curves could be constructed according to the frequency-temperature superposition principle⁵ with respect to two reference temperatures, i.e., $T_{\text{ref}} = 18^\circ\text{C}$ (io) and $T_{\text{ref}} = 30^\circ\text{C}$ (nio).

Results and Discussion

Typical plots of storage moduli $G'(\omega)$ are shown in Figures 3 and 4. The sample in Figure 3 was a microemulsion with an ionic surfactant, and in Figure 4 a nonionic surfactant system was used. In the following we discuss the storage modulus only. This material function is more sensitive to the changes of the structure of our systems that have a considerable influence on the mechanical properties. In Figures 5 (ionic) and 6 (nonionic) the master curves of $G'(\omega)$ are shown for different polymer concentrations. The corresponding shift factors a_T for the ionic microemulsion samples are plotted in Figure 7 as functions of the reciprocal temperature, showing their Arrhenius-like behavior. It is important to note that the discussion is restricted to the high-frequency relaxation process and its characteristic relaxation time (τ_{m1}) and plateau modulus (G_{P1}).

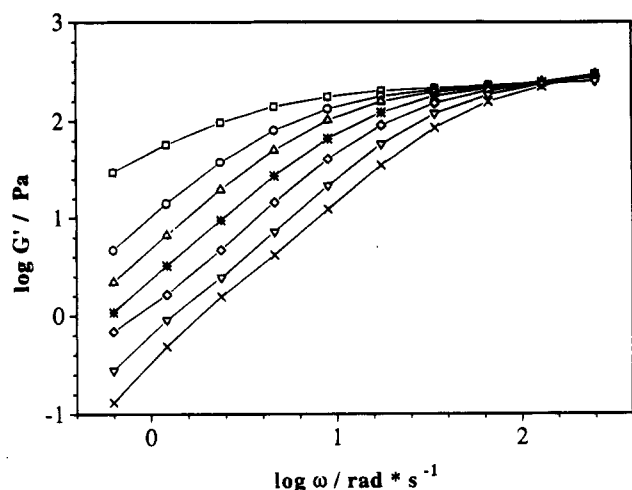


Figure 3. Storage moduli G' of the ionic microemulsion (polymer concentration: $R = 4$): (\square) 278, (\circ) 279, (Δ) 280, ($*$) 281, (\diamond) 282, (∇) 283, (\times) 284 K.

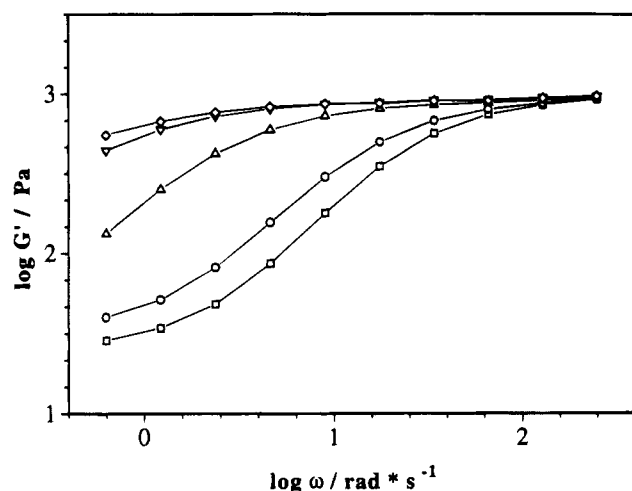


Figure 4. Storage moduli G' of the nonionic microemulsion (polymer concentration: $R = 4$): (\diamond) 309, (∇) 305, (\circ) 303, (\square) 301 K.

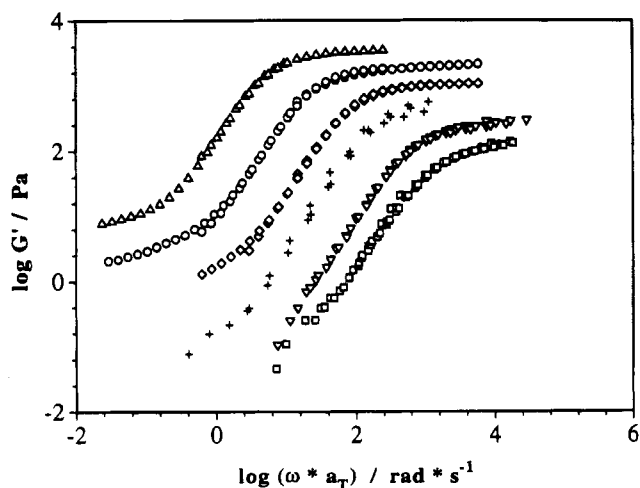


Figure 5. G' master curves of the ionic microemulsion in dependence of polymer concentration at $T_{\text{ref}} = 18^\circ\text{C}$: (\square) $R = 3$, (∇) $R = 4$, ($+$) $R = 6$, (\diamond) $R = 8$, (\circ) $R = 12$, (Δ) $R = 20$.

It is apparent that both systems show qualitatively similar mechanical behavior. The temperature dependence of the isotherms, however, is opposite: the storage modulus $G'(\omega)$ at a fixed frequency increases with temperature in the system with a nonionic surfactant

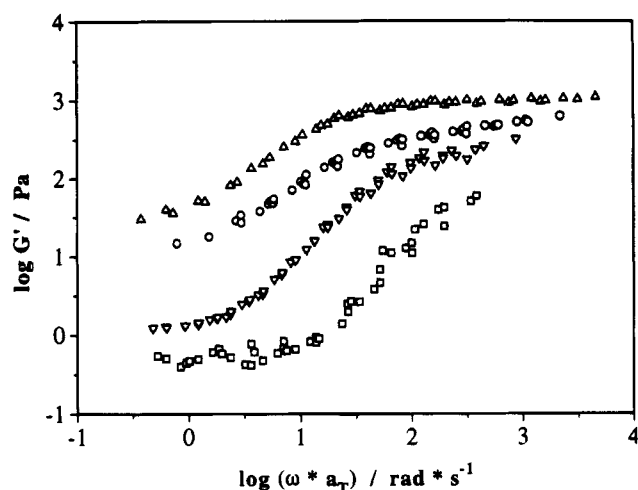


Figure 6. G' master curves of the nonionic microemulsion in dependence of polymer concentration at $T_{\text{ref}} = 30^\circ\text{C}$: (\square) $R = 1$, (∇) $R = 2$, (\circ) $R = 3$, (Δ) $R = 4$.

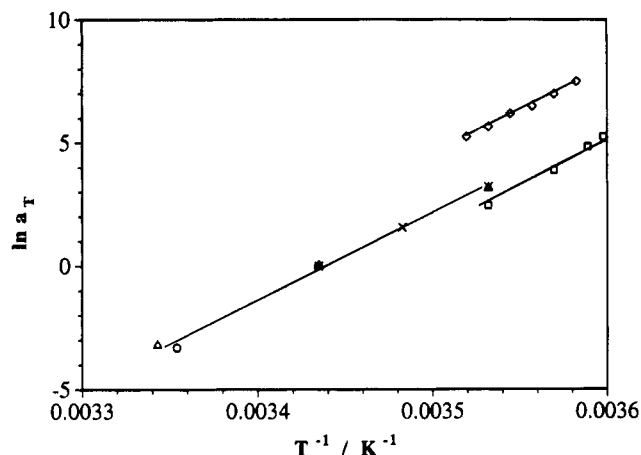


Figure 7. Arrhenius plots of the shift factors a_T of the ionic microemulsion series for different polymer concentrations R (reference temperature $T_{\text{ref}} = 18^\circ\text{C}$): (\square) $R = 3$, (\diamond) $R = 4$, (\times) $R = 8$, (Δ) $R = 12$, (\circ) $R = 20$.

and decreases if an ionic amphiphile is used. This observation can be understood by considering the temperature-dependent phase behavior of the underlying microemulsions. It is well-known that temperature variation causes reversible nanodroplet aggregation in microemulsions, eventually resulting in the formation of an infinite cluster of nanodroplets. This phenomenon can be explained in terms of a percolation-like transition. The tendency of individual water globules (of given size and concentration) to aggregate is raised with increasing temperature for microemulsions stabilized by ionic surfactants and, in contrast, with decreasing temperature for nonionic surfactant systems. It is essential to note that this phase behavior of our microemulsions is virtually preserved for the cross-linked systems containing block copolymers.⁶

To understand the influence of the phase behavior on the mechanical properties, we have to keep in mind that the network cross-links are formed by nanodroplets and their solubilized POE blocks (see Figure 1). Two effects can be anticipated if nanodroplets form clusters: approaching the infinite cluster transition temperature (T_c), the time of droplet-droplet contact grows. This favors the exchange of POE blocks between nanodroplets and, consequently, lowers the lifetime of network cross-links. Moreover, the formation of droplet clusters disturbs the structure of the whole transient network,

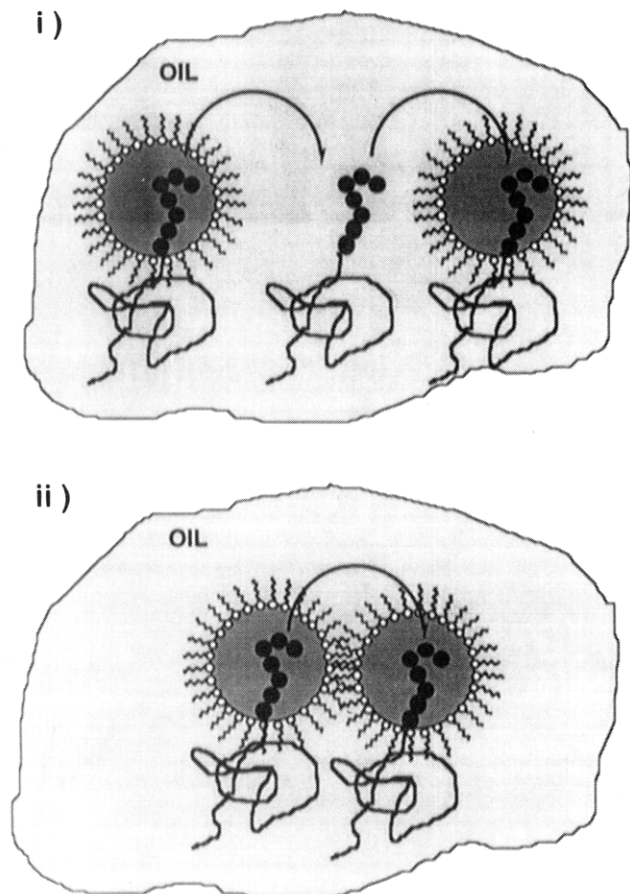


Figure 8. Two mechanisms of POE exchange between nanodroplets: (i) across the surrounding oil phase; (ii) during droplet-droplet contact.

because nanodroplets involved in cluster formation are not available as network cross-links.

Depending on temperature, composition, and the chemical nature of the surfactant, we have to distinguish two possible mechanisms determining the lifetime of network cross-links in the experimentally accessible temperature region: exchange of network links between nanodroplets (i) across the surrounding oil phase and (ii) during collision of two nanodroplets (see Figure 8). Whereas the first mechanism is expected to occur at low droplet concentrations and/or far away from T_c , the second mechanism (ii) should prevail at higher droplet concentrations and/or approaching T_c .

As long as viscoelastic behavior is controlled by the activation process of disruption of POE blocks from nanodroplets associated with mechanism i, an Arrhenius-like temperature dependence is to be observed. The slope of the plots in Figure 7 yields the activation energy E_a in the ionic surfactant system. According to this figure, E_a is about 300 ± 50 kJ/mol and appears to be independent of R , indicating that the underlying process is the disruption of a single network link. Note that the experiments were carried out in the dilute concentration range; only the highest polymer concentrations ($R \geq 12$) exceed the overlap concentration of the individual blocks.⁷

We intend to discuss this process analogously to the analysis of adhesion promoters⁸ which (we think) helps us to clarify the physical situation. Disruption of a network link occurs via PI chains which are stretched up to a final length l_f . When the droplet-droplet distance exceeds l_f , the chain snaps back into the

random-coil conformation and dissipates some energy: this is the leading contribution to E_a .

An important observation is that POE blocks can be pulled out of the nanodroplets only when the force acting on them is beyond a certain threshold f^* . There are two main contributions to f^* : α , the POE transfer from a good solvent (=water) into a poor one (=oil) corresponding to an energy $\Delta\mu$, and β , the reduced entropy of the PI midblock.

We represent f^* as a geometric mean between both contributions, i.e.,

$$f^* = (k_B T \Delta\mu)^{1/2} / b \quad (3)$$

where b is the Kuhn length (length of an elastically active unit). Since $\Delta\mu \approx k_B T$, eq 3 simplifies to

$$f^* \approx \Delta\mu / b \quad (4)$$

The other important quantity is the ultimate length l_f in the regime $\Delta\mu \approx k_B T$ the chains are nearly fully extended and, consequently,

$$l_f \approx Nb \quad (5)$$

where N is the degree of polymerization of the PI midblock.

The energy E_a is then simply the work to pull out the POE chain with a force f nearly equal to the threshold value f^* :

$$E_a \sim f^* l_f = f^* Nb = N \Delta\mu \quad (6)$$

The POE group disconnects from the aqueous core of the nanodroplet as soon as each elastically active unit of the attached PI chain has acquired an energy comparable to $\Delta\mu$. This energy is stored in the PI midblock. After scission an energy proportional to $N \Delta\mu$ is dissipated; hence, the experimentally determined activation energy E_a is proportional $N \Delta\mu$.

For illustration we determine an order of magnitude of $\Delta\mu$ by inserting $N = 735$ for the PI midblocks of our triblock copolymers: $\Delta\mu_{io}$ turns out to be about 400 J/mol for the ionic microemulsion series. This figure enables us to make a guess of the equilibrium number of active chains in the network, ν_0 :

$$\nu_0 = \frac{\exp(\Delta\mu/k_B T)}{1 + \exp(\Delta\mu/k_B T)} n \quad (7)$$

where n is the total number of triblock copolymer chains.³ For the ionic surfactant system we find $\nu_{0io} = 0.54n$.

Later in this paper we will be able to obtain (contrary to this procedure) an experimental value of $\Delta\mu_{io}$ from the R -dependence of the lifetimes of POE blocks in the aqueous core of the nanodroplets.

In the case of the nonionic microemulsion series the existence region is limited to $\Delta T \approx 10$ K; i.e., the temperature region is too small to determine $\Delta\mu_{nio}$ directly from α_T .

Approaching T_c in microemulsions, the lifetimes of nanodroplet aggregates increase. In this state POE groups of network chains can be exchanged easily between nanodroplets during droplet-droplet collisions because the time of a droplet-droplet contact is long enough to allow exchange mechanism ii. This is clearly

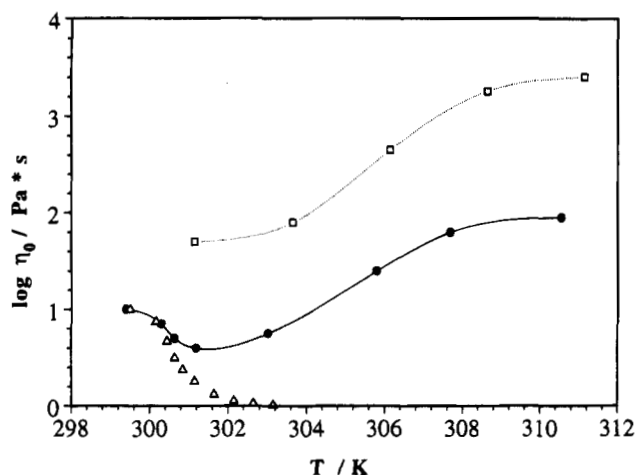


Figure 9. Characteristic viscosities of the nonionic series for different polymer concentrations: (Δ) $R = 0$ (pure microemulsion), (\bullet) $R = 2$, (\square) $R = 4$.

demonstrated in Figure 9, where characteristic viscosities η associated with the high-frequency relaxation process are plotted as a function of T for $R = 2$ and $R = 4$ of the nonionic microemulsion. For illustrative purposes the viscosity of the pure nonionic microemulsion ($R = 0$) is included. This microemulsion shows a remarkable viscosity increase with decreasing temperature, indicating the formation of a system-spanning nanodroplet cluster.⁶ At low polymer concentrations this nanodroplet cluster controls the viscosity of block copolymer containing microemulsions within the temperature region around T_c . This is apparent from the coincidence of the viscosities for the samples with $R = 0$ and $R = 2$. With increasing temperature the droplet cluster redisperses and the thermoreversible network formation is mirrored by a rise of η of more than 2 decades.

To study the influence of varying triblock copolymer concentrations in the two different microemulsions (ionic or nonionic), one has to refer to isothermal conditions. In Figures 5 and 6 the plateau moduli G_{P1} and the relaxation times τ_{m1} at higher frequencies could be well determined by using an empirical equation.¹¹

Also the limiting low frequencies of the high-frequency relaxation process were derived from Figures 5 and 6. Independent of R and the particular surfactant, the storage moduli can be matched by $G' \sim \omega^{1.4 \pm 0.2}$. This is in qualitative agreement with theoretical predictions by Tanaka and Edwards.³ These authors suggested that the slopes of $G'(\omega)$ are smaller for transient networks in the characteristic relaxation zone as compared to the corresponding functions of other viscoelastic materials, e.g., polymer melts. A reason for this deviation might be seen in the lifetimes of our transient network cross-links, which are dependent on the end-to-end distance of the network links.

The master curves of Figures 5 and 6 permit one to derive the high-frequency plateau moduli G_{P1} as a function of R (see Figure 10), showing that G_{P1} grows linearly with R . The G_{P1} plot for the nonionic series intersects the R -axis at $R \approx 1$. Since the number of network cross-links, i.e., the number of nanodroplets, stays constant within one type of microemulsion, a rise of R increases the formal functionality Φ of the cross-links; $R \approx 1$ corresponds to $\Phi \approx 2$. For our systems a threshold concentration corresponding to a mean functionality of $\Phi = 2$ has to be expected, where a system-spanning spatial network is formed.

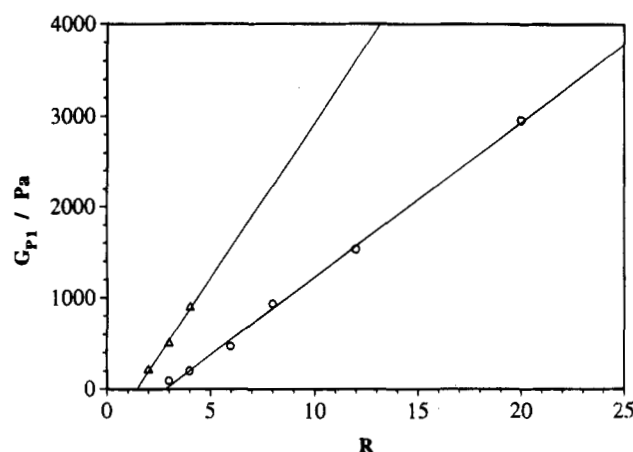


Figure 10. High-frequency plateau moduli G_{P1} plotted against polymer concentration R for the ionic (\circ) and the nonionic (Δ) series.

Opposite to the just-discussed nonionic system, the samples based on the ionic microemulsion show a larger threshold concentration of block copolymers necessary to build up viscoelastic networks, i.e., $R \approx 3$ (or $\Phi \approx 6$). This "retarded" network formation requires a larger threshold equilibrium polymer concentration before the ABA triblock copolymers are able to form network links. In order to understand this peculiar difference between the two microemulsion systems, differing only by the kind of surfactant, one has to inspect the specific polymer surfactant interactions of both systems.

It is a well-known phenomenon that POE is adsorbed strongly onto an interface built up by ionic surfactants.⁹ Consequently, POE blocks dissolved in the microemulsion are either adsorbed at the oil/water interface or dissolved via a solvation by AOT molecules in the oil continuum. Both states of POE have nearly equal probabilities, and such POE blocks do not contribute to the formation of elastically active chains. As soon as the oil/water interface is saturated by POE, further hydrophilic blocks can be dissolved in the aqueous core of nanodroplets, forming a three-dimensional microemulsion-polymer network. These considerations conform well with PFG-NMR results of our ionic systems.¹⁰ Such experiments revealed that the self-diffusion coefficients of surfactant and triblock copolymer molecules are almost identical and indicate that their diffusive transport is strongly correlated.

In the case of a nonionic surfactant (with a polar headgroup consisting of ethylene oxide units) forming a "brush" at the oil/water interface, the POE/surfactant interactions are repulsive,⁹ thus forcing POE blocks into the water core of the nanodroplets. Due to these repulsive interactions, the nonionic surfactant cannot solvate POE blocks in the oil phase opposite to AOT molecules. Thus, the energy difference must be larger between POE in the water pool and the oil phase in the nonionic system compared to the case of the AOT microemulsion (see above). Also the lifetimes of network links in a nanodroplet of ionic and nonionic microemulsions should be different. Since the relative numbers of active chains ν_0 for both systems are known, these different lifetimes can be derived—to first order—from the slopes of $G_{P1}(R)$ -plots in Figure 10:³

$$G_{P1} = \nu_0 k_B T \tau \quad (8)$$

where τ is the lifetime of a network cross-link. Because of the specific surfactant/polymer interactions, the non-

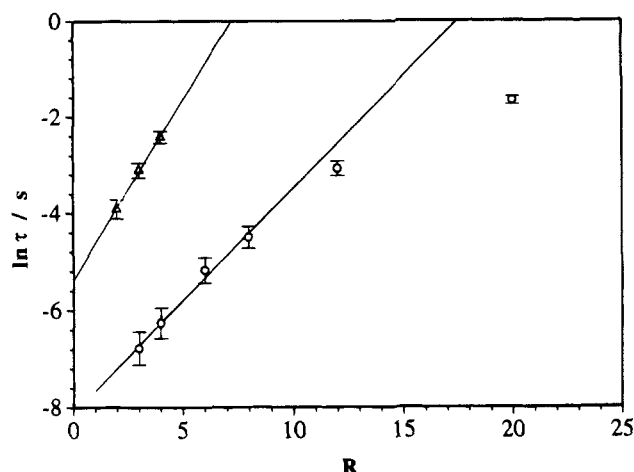


Figure 11. Lifetimes τ of network cross-links plotted against polymer concentration R for the ionic (\circ) and the nonionic (Δ) microemulsion series.

ionic samples show a steeper slope, indicating that the lifetime of a network link is larger than that in the ionic series.

The individual residence times of POE blocks in nanodroplets control the lifetimes of network cross-links which are related to the high-frequency relaxation times τ_{m1} . They can be determined from the master plots shown in Figures 5 and 6; τ_{m1} increases with R . This is plausible because of the special structure of these microemulsion-based transient networks; an increase of R affects only the functionality Φ of the cross-links since the number of network junctions (=number of nanodroplets) stays constant.

The terminal relaxation time τ_{m1} is proportional to the lifetime of a network cross-link τ , where

$$\tau = \tau_0 \exp(\Delta\mu/k_B T) \quad (9)$$

$\Delta\mu$ is the heat of POE transference and τ_0 the lifetime for $\Delta\mu = 0$. The transference of R POE blocks is assumed to be $R\Delta\mu$ —to first order, i.e., independent of R :

$$\frac{\Delta\mu R}{k_B T} = \ln\left(\frac{\tau}{\tau_0}\right) \quad (10)$$

Introducing the activity a_{POE} of solubilized POE blocks in the aqueous core of the nanodroplets by

$$\mu = \mu^0 + kT \ln a_{\text{POE}} \quad (11)$$

one arrives at

$$\tau/\tau_0 = a_{\text{POE}}^R \quad (12)$$

a general exponential function with $a_{\text{POE}} > 1$.

A semilogarithmic plot of eq 10 ($\ln(\tau)$ against R) yields the heat of transference $\Delta\mu$ for small values of R (see Figure 11). Samples of the ionic microemulsion show deviation from the linear behavior for $R \geq 12$ due to

increasing polymer–polymer interactions while exceeding their overlap concentration.⁷

From Figure 11 we get $\Delta\mu_{\text{io}} = 1150$ J/mol and $\Delta\mu_{\text{ni}} = 1860$ J/mol. The ratio $\tau_{\text{io}}^0/\tau_{\text{ni}}^0$ turns out to be about 10. Opposite to the situation discussed earlier ($\Delta\mu_{\text{io}} = 400$ J/mol), we possess now an experimental value of $\Delta\mu_{\text{io}}$ which allows us to derive N , the proportionality factor in eq 6. This procedure suggested that we define a persistence length b (corresponding to the Kuhn length) to be $b \approx 3l_{\text{mon}}$, i.e., 3 times the length of a monomeric unit (l_{mon}) of a triblock copolymer molecule.

Conclusions

We think that we obtained an interesting collection of rheologic data. They could be related to molecular processes in transient networks formed by triblock copolymers dissolved in ionic and nonionic water-in-oil microemulsions. Such process are believed to be responsible for the viscoelastic behavior of these complex materials. Further (dynamic) data from quasielastic light scattering measurements will soon be available, from which detailed information on diffusional motions of nanodroplets and triblock copolymers can be extracted.

Acknowledgment. The authors are grateful to Drs. Chr. Friedrich (FMF, Freiburg, FRG) and F. Stieber for valuable discussions. They also acknowledge help with the experiments by H. Hammerich and Y. Hauger. This work was supported by the Swiss National Science Foundation.

References and Notes

- (1) de Gennes, P.-G.; Taupin, C. *J. Phys. Chem.* **1982**, *86*, 2294.
- (2) Jouffroy, J.; de Gennes, P.-G. *J. Phys. (Les Ulis, Fr.)* **1982**, *43*, 1241.
- (3) Borkovec, M.; Eicke, H. F.; Hammerich, H.; Das Gupta, B. *J. Phys. Chem.* **1988**, *92*, 206.
- (4) Green, M. S.; Tobolsky, A. V. *J. Phys. Chem.* **1946**, *14*, 80.
- (5) Baxandall, L. G. *Macromolecules* **1989**, *22*, 1982.
- (6) Tanaka, F.; Edwards, S. F. *Macromolecules* **1992**, *25*, 1516.
- (7) Tanaka, F.; Edwards, S. F. *J. Non-Newtonian Fluid Mech.* **1992**, *43*, 247–309.
- (8) Eicke, H.-F.; Quillet, C.; Xu, G. *Colloids Surf.* **1989**, *36*, 97.
- (9) Quillet, C.; Eicke, H.-F.; Hauger, Y. *Macromolecules* **1990**, *23*, 3347.
- (10) Eicke, H.-F.; Hilfiker, R.; Xu, G. *Helv. Chim. Acta* **1990**, *73*, 213.
- (11) Struis, R. P. W. J.; Eicke, H.-F. *J. Phys. Chem.* **1991**, *95*, 5989.
- (12) Vollmer, D.; Hofmeier, U.; Eicke, H.-F. *J. Phys. II* **1992**, *2*, 1677.
- (13) Zölzer, U.; Eicke, H.-F. *J. Phys. II* **1992**, *2*, 2207.
- (14) Vinogradov, G. V.; Malkin, A. Ya. *Rheology of Polymers*; Mir Publishers: Moscow, 1980.
- (15) Meier, W.; Odenwald, M.; Fedtke, B.; Eicke, H.-F. Presented at the 5th European Polymer Federation Symposium on Polymeric Materials (EPF), Basel, Switzerland, Oct 1994.
- (16) Brandrup, J.; Immergut, E. H., Eds. *Polymer Handbook*, 3rd ed.; Wiley and Sons: New York, 1989.
- (17) Brochard-Wyart, F.; de Gennes, P.-G.; Lèger, L.; Marciano, Y.; Raphael, E. *J. Phys. Chem.* **1994**, *98*, 9405.
- (18) Raphael, E.; de Gennes, P.-G. *J. Phys. Chem.* **1992**, *96*, 4002.
- (19) de Gennes, P.-G. *J. Phys. Chem.* **1990**, *94*, 8407.
- (20) Cabane, B.; Duplessix, R. *J. Phys. Chem.* **1982**, *43*, 1529.
- (21) *Colloids Surf.* **1985**, *13*, 19.
- (22) *J. Phys.* **1987**, *48*, 651.
- (23) Kabalnov, A.; Olsson, U.; Wennerström, H. *Langmuir* **1994**, *10*, 2159.
- (24) Stieber, F.; Hofmeier, U.; Eicke, H.-F.; Fleischer, G. *Ber. Bunsen-Ges. Phys. Chem.* **1993**, *97*, 812.
- (25) Fleischer, G.; Stieber, F.; Hofmeier, U.; Eicke, H.-F. *Langmuir* **1994**, *10*, 1780.
- (26) Friedrich, C.; Braun, H. *Rheol. Acta* **1992**, *31*, 309.

MA950127M